

Trading-off Accuracy and Communication Cost in Federated Learning

Mattia Jacopo Villani
King’s College London
London, United Kingdom
mattia.villani@kcl.ac.uk

Emanuele Natale
Université Côte d’Azur
Sophia-Antipolis, France
emanuele.natale@univ-cotedazur.fr

Frederik Mallmann-Trenn
King’s College London
London, United Kingdom
frederik.mallmann-trenn@kcl.ac.uk

ABSTRACT

Leveraging the training-by-pruning paradigm introduced by Zhou et al. [NeurIPS’19], Isik et al. [ICLR’23] introduced a federated learning protocol that achieves a 34-fold reduction in communication cost. We achieve a compression improvements of orders of orders of magnitude over the state-of-the-art. The central idea of our framework is to encode the network weights \vec{w} by a the vector of trainable parameters \vec{p} , such that $\vec{w} = Q \cdot \vec{p}$ where Q is a carefully-generate sparse random matrix (that remains fixed throughout training). In such framework, the previous work of Zhou et al. [NeurIPS’19] is retrieved when Q is diagonal and \vec{p} has the same dimension of \vec{w} .

We instead show that \vec{p} can effectively be chosen much smaller than \vec{w} , while retaining the same accuracy at the price of a decrease of the sparsity of Q . Since server and clients only need to share \vec{p} , such a trade-off leads to a substantial improvement in communication cost. Moreover, we provide theoretical insight into our framework and establish a novel link between training-by-sampling and random convex geometry.

KEYWORDS

training-by-pruning, communication-efficient federated learning, parameter sharing, networks with random weights, compression, random convex geometry, zonotopes

1 INTRODUCTION

In many scenarios, training cannot be done on a single machine, either due to the large size of the dataset or privacy concerns that prevent direct data sharing (e.g., hospital data). To enable efficient and secure training on mobile devices, *federated learning* was introduced [15, 20]. In this approach, multiple agents or clients train on separate partitions of the data, periodically sharing learned parameters with a central server. The server aggregates these parameters and distributes the updated model back to all clients.

In this server-client framework the training data is split across many clients who, with the help of a central server, jointly train a model without ever sharing data directly. A well-known example is [8], which demonstrates that federated learning for next-word prediction on virtual keyboards significantly improved recall compared to centralized training on lower-quality data. Furthermore, the distributed computation across clients can accelerate training.

However, the main issue of this framework is that it requires the model (i.e., all learnable parameters) to be frequently shared with all clients resulting in a very high communication cost. Communicating large amounts of data slows down training significantly. To address this issue [13] proposed a novel framework that allows the clients to simply share one bit (rather than a float) per parameter of the model. This results in a 32-fold reduction in communication

cost.¹ Their work builds on the training-by-pruning paradigm introduced by [31]. In this paradigm, instead of applying gradient descent on a fixed collection of weights, weights are randomly initialised and removed with some probability that changes adaptively. Specifically, each randomly initialised parameter (weight) w_i has an associated probability p_i of being used in the neural network architecture. During training, we sample every weight, and with probability $1 - p_i$, the weight gets a value of 0. The goal then is to use gradient-based methods to train the distribution of \vec{p} for each p_i ,² so that the sampled network has minimal loss. Surprisingly, this seems to work very well in practice, leading to the development of other variants, such as, the Edge-PopUp algorithm by [23].

In federated learning, transmitting binary masks instead of exact parameter values not only reduces communication cost but also enhances privacy. Additionally, the sparse network architecture lowers inference costs. Using this technique, [13] achieved high accuracy in training artificial neural networks (ANNs) with a 32-fold communication reduction. They further applied compression techniques that capitalize on patterns of consecutive 1s or 0s, yielding a total communication reduction of 33-34 times.

Our paper extends far beyond this 34-fold reduction in communication cost, achieving a 1024-fold total reduction. The idea is that the clients and server jointly (from a shared random seed) initialise a sparse *coefficient matrix* Q where each row has d -non zero parameters.

The trainable parameters are given by a n -dimensional probability vector \vec{p} with $n \ll m$, where m is the total number of parameters of the model. Each client k samples a binary vector $z^{(k)} \sim \text{Bern}(\vec{p})$, where $\text{Bern}(\vec{p})$ is the component-wise Bernoulli distribution. Each client then calculates its weights as follows $\vec{w}^{(k)} = Qz^{(k)}$.³ After calculating the local gradient, each client then updates \vec{p} to \vec{p}_{new} and samples once more $z_{new}^{(k)} \sim \text{Bern}(\vec{p}_{new})$ before sending it to the server. Crucially, sending $z_{new}^{(k)}$ takes at most n bits which can be orders of magnitude smaller than m (see [13])⁴ and much smaller than sending float values to the server which would cost $32m$. Fascinatingly, when sending n bits vs $32m$ bits we only see (Figure 4) a very small decrease in accuracy up to a certain threshold of n . When n becomes too small, the model starts to deteriorate (Figure 3). However, for example in the case of MNIST, n can be

¹Their model still requires the server to share the a float for every parameter.

²Technically, one trains via SGD a score value s_i from when then the p_i is calculated: $p_i = \text{sigmoid}(s_i)$ to ensure that the values of p_i are in $[0, 1]$.

³Note that this model is different from parameter sharing as potentially all weights/parameters can be different. There is some correlation between each parameter, but ultimately it fairly weak and results in high accuracies as we show in our experiments (see Section 3).

⁴As mentioned before, they also use some other forms of compression when the binary vector has many 0s or 1s, but the savings are negligible in the grand scheme of things.

smaller than m by a factor of 32 and we only lose a 7 percent points of accuracy - giving a total compression of $32 \cdot 32 \approx 1024$.

In some sense, the framework of [13] (building on training-by-pruning from [31]) is a special case of our model when $d = 1$ and $n = m$.⁵ It turns out that allowing larger values of d increases accuracy. In Section 2.1 we discuss the reasons for this. Typically, in federated learning, the communication complexity is measure by the communication each clients needs to send, but it's easy to see that a low server communication cost can also be crucial. In [13] and our main algorithm, the server still broadcasts the entire model. However, in our approach that cost is only $32n$ vs $32m$, which, as argued above, can be smaller by an order of magnitude without losing too much accuracy.

Although we frame our results in the setting of federated learning, the model itself is also interesting to understand the impact dimension reduction w.r.t. the learnable parameters. For this reason we also introduce the LOCAL ZAMPLING algorithm in Section 1.3 a simplified local version of the algorithm outside of the context of federated learning. Here, we study the generalisation of the learned vector \vec{p}^* . Finally, we complement our experiments with theoretical results on the rich convex random geometry (namely zonotopes) induced by our framework.

1.1 Our Contribution

We present ZAMPLING (Zonotope Sampling), a new training-by-sampling framework inspired by convex random geometry that achieves small reductions in accuracy for state of the art factors of compression in communication cost in the federated learning setting. Given an arbitrary neural network architecture, ZAMPLING replaces the model's parameters \vec{w} with a product of a probability vector \vec{p} and a sparse influence matrix Q , enabling both training-by-sampling for any model and state of the art compression in parameter communication costs in the federated setting. Our framework enables large parameter compression that lowers the communication cost by several orders of magnitude in the context of Federated Learning: FEDERATED ZAMPLING. Moreover, our work is a generalisation of Zhou et. al. [31] and sheds novel theoretical insight on the generalisation benefits from training-by-sampling. We now give an overview of our contributions.

Highly Compressed Communication Cost in Federated Learning Our main result shows that we can reduce the client communication cost by a factor of 1024 in comparison to the naïve algorithm (and a factor of 32 w.r.t. the state-of-the-art) while witnessing only a 3% point reduction in accuracy. We also provide theoretical insights into why federated learning is helpful in our setting (Section 2.3.2). Moreover, we achieve a fine-grained Trade-off between accuracy and compression for LOCAL ZAMPLING. In Section 3.1 we perform numerical experiments on a small architecture (to avoid redundancy in parameters). We show a relatively smooth trade-off between accuracy and compression factor. Our results also show that increasing d slightly benefits higher accuracy, but large values of d yield no additional benefits.

⁵There are some minor difference, technically Q would be a diagonal matrix and the scores are calculated using the sigmoid function rather than our clipping, but overall it is virtually the same. Crucially, since $n = m$ no further compression can be obtained.

Theoretical Foundations of Training-by-Sampling and a Novel Link to Random Convex Geometry. We provide theoretical evidence on the benefits of deploying training-by-sampling algorithms in the federated setting (see Section 2). First we show what the impact of d is. We argue in Proposition 2.4 that the expected maximum norm of $Q_i \vec{p}$ scales as $\Theta(\sqrt{d/n_\ell})$ where the maximum is taken over \vec{p} . This implies that for larger values of d the model can reach larger weights. We also show characterize the number of 0 entries in $\vec{w}(0)$ and $\vec{0}$ columns in Q that can arise for small d and may limit the expressivity of the model. See Section 2.1 for the details. In Section 2.3 we develop a novel link with random convex geometry that allows us to prove statements about the generalisation capabilities of training-by-sampling. This allows us then to prove the benefits on federated learning has when it comes to learning by sampling (see Section 2.3.2).

Through our formalism (Section 2.3), and experimentally (Section 3.3), we provide evidence that training-by-sampling improves generalisation. This is because our method can be described as searching for good solutions on the vertices of a convex shape known as a zonotope. Through training, the algorithm finds a sub-zonotope where performance is good. Even though our training method only measures performance at the vertices of this shape, we show experimentally that good performance is maintained in all the region characterised by the shape, comparing it to gradient-based training Section 3.3. Finally, our findings (see Figure 5) show that when training the sampled network instead of simply training \vec{p} directly without ever sampling, then the network does not generalise as well and suffers a huge drop of accuracy, to which we refer as the *integrality gap*.

1.2 Related Work

There is long line of research on communication efficient federated learning. The authors of [1] achieve a reduction in communication cost by only exchanging the largest gradients. In a similar spirit, [2] also estimates the SGD update and [17] sparsifies the gradients to optimize for bandwidth usage. [14] present an algorithm and theoretical foundations on sparsification using successive refinement. Other methods that build on low-rank approximation include [29] and [3]. Our work extends this by showing that an even smaller set of parameters can be shared while maintaining accuracy.

Other approaches to reducing communication costs include parameter sharing schemes like those proposed by [5] and [2], which aim to minimize communication through compressed updates or estimating SGD steps. Similarly, [26] explored the use of shared randomness to achieve lossless communication compression. Our approach draws on similar principles but extends these ideas by combining the use of sparse random matrices and convex geometry insights.

Up to minor difference, that the special case $n = m$ and $d = 1$ is akin to the training-by-pruning algorithm considered in [31]. Said algorithm motivated the Strong Lottery Ticket Hypothesis [22], and other training-by-pruning algorithms such as Edge-PopUp [24]; finding lottery tickets has been shown to be computational difficult [7, 21]. It also found applications in federated learning for distributed training of neural networks with reduced communication cost [13].

Recent papers demonstrate a strong focus on advancing federated learning techniques, particularly in contexts involving data heterogeneity and decentralized environments. For example, the AAMAS papers (2023-2024) [10] introduces attention mechanisms to address the aggregation challenges inherent in federated reinforcement learning across heterogeneous agents. Similarly, the study [27] explores methods to handle non-i.i.d. data by clustering clients with similar distributions prior to aggregation, thereby improving model accuracy and robustness.

Finally, if side information is available, the authors of [12] use sampling to achieve a 2650-fold compression in the context of federated learning. Moreover, shared randomness has been successfully used to reduce the communication cost, e.g., [4, 11, 16]. Our method achieves a 1024-fold reduction in communication cost.

1.3 Our Framework: ZAMPLING

We consider the setting of federated learning, where a server and K clients jointly train a neural network model. For any neural network architecture, let m be the total number of parameters of the model and let n be a number of *trainable parameters* with $n \leq m$. Let $\vec{p}(t) \in [0, 1]^n$ be the vector of these parameter at time t and we refer to it as the *probability distribution vector*.

Let $Q = (q_{i,j})_{i \leq m, j \leq n}$ be a randomly initialised but non-trainable matrix $\in \mathbb{R}^{m \times n}$ that describes how each trainable parameter (in \vec{p}) affects each weight, i.e., $q_{i,j}$ describes how the j th trainable parameter influences the i th weight. Let d the weight degree (each weight is influenced by d trainable parameters), i.e., the number of non-zero entries per row. The matrix Q does not change over time and will never be sent – we assume that server and clients both have Q which can be realised by sharing the same random seed to generate identical matrices. We assume that the data is distributed IID among the clients.

Further Notation. Let $f(x) = \max(\min(x, 1), 0)$ be the ReLU function clipped at 1. Let $D_{(k)}$ be the dataset at agent $k \leq K, k \in \mathbb{N}$ and $D = \bigcup_{k \leq K} D_{(k)}$. Given a weight vector \vec{w} , we use $g_{\vec{w}} : X \rightarrow Y$ to describe the resulting network (note that server and clients use the same architecture and hence the weight vector fully determines the model). We define the *compression factor* to be m/n . In our terminology each *round* has up to 100 (training) epochs. Clients and server exchange messages at the beginning and end of each round.

Initialization. We generate a coefficient matrix $Q \in \mathbb{R}^{m \times n}$. For each $i \leq m$ sample a set of d indices $\mathcal{I}_i \in [n]^d$ without replacement. Then generate Q as follows.

$$q_{i,j} \sim \begin{cases} N(0, \sigma_i^2) & \text{if } j \in \mathcal{I}_i \\ 0 & \text{otherwise} \end{cases}, \quad (1)$$

where $\sigma_i^2 = \frac{6}{dn_\ell}$ and n_ℓ is the fan-in (number of incoming weights) of the target neuron associated to weight w_i (see Lemma 2.1 where we show that this results in a Kaiming-He initialization).

The initial values of \vec{p} are drawn from an n -dimensional uniform distribution $\vec{p}(0) \sim U(0, 1)^n$. The initial values of the weights are now calculated by setting $\vec{w}_{init} = \vec{w}(0) = Q\vec{p}(0)$.

LOCAL ZAMPLING (Centralized Version). We start by describing the LOCAL ZAMPLING framework/algorithm, which trains the model

locally on one central machine (not in the federated learning framework). In each round t :

- Set $\vec{s}(t) = \vec{p}(t)$
- Sample the binary mask $\vec{z}(t) \in \{0, 1\}^n: \vec{z}(t) \sim \text{Bernoulli}(\vec{p}(t))$
- Calculate the weights vector⁶ $\vec{w}(t) = Q \cdot \vec{z}(t)$.
- $\vec{w}(t)$ is used for the forward pass, and the loss $\mathcal{L}(g_{\vec{w}(t)}, D)$ is backpropagated to update the score mask as $\vec{s}(t+1) = \vec{s}(t) - \eta \nabla \mathcal{L}(g_{\vec{w}(t)}, D)$ (η is the learning rate).

Note that this training method ensures that the sampled networks achieve good performance, as we discuss in Section 3; this is not the case if we train the same architecture traditionally (without sampling throughout training), as we discuss in Appendix A, where we relate the sampled versus non-sampled gap in the network’s performance to the initialisation of \vec{p} .

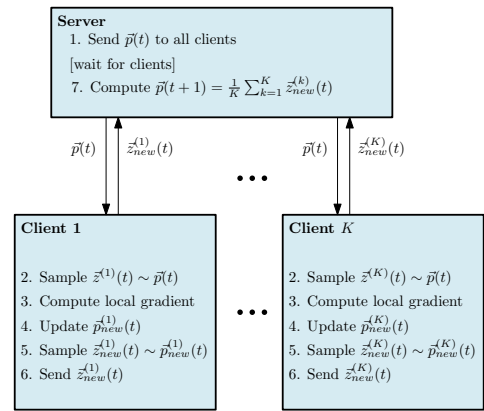


Figure 1: An illustration of the FEDERATED ZAMPLING algorithm.

FEDERATED ZAMPLING (Federated Learning Version). We now describe the FEDERATED ZAMPLING (see Section 1.3 for an illustration of the protocol). For the initialisation, it is important that both server and clients have Q . This can be realised by building Q through using a shared random number generator. In each round t :

- The server sends $\vec{p}(t)$ to all its clients (as a float).
- Each client k calculates $\vec{s}^{(k)}(t) = \vec{p}(t)$
- Each client k samples the binary mask $\vec{z}^{(k)}(t) \in \{0, 1\}^n$ as follows $\vec{z}(t) \sim \text{Bernoulli}(\vec{p}(t))$
- Each client calculates its local weights as a vector $\vec{w}^{(k)}(t) = Q \cdot \vec{z}^{(k)}(t)$
- $\vec{w}(t)$ is used for the forward pass, and the loss $\mathcal{L}(g_{\vec{w}^{(k)}(t)}, D_k)$ on the local task is backpropagated to update the score mask at client k as $\vec{s}_{new}^{(k)}(t) = \vec{s}^{(k)}(t) - \eta \nabla \mathcal{L}(g_{\vec{w}^{(k)}(t)}, D_k)$ (η is the local learning rate).
- Each client k converts the score back to probabilities: $\vec{p}_{new}^{(k)}(t) = f\left(\vec{s}_{new}^{(k)}(t)\right)$
- Each client samples from this $\vec{z}_{new}^{(k)}(t) \sim \text{Bernoulli}(\vec{p}_{new}^{(k)}(t))$ and sends $\vec{z}_{new}^{(k)}(t)$ to the server.

⁶We assume that clients and server have the same mapping of entries in this vector to weights in the architecture.

- The server calculates $\vec{p}(t+1) = \frac{1}{K} \sum_{i=k}^K \vec{z}^{(k)}(t)$.

Sometimes we will also compare to the ContinuousModel, where no sampling happens, i.e., $\vec{w}^{(k)}(t) = Q\vec{p}(t)$ instead of $\vec{w}^{(k)}(t) = Q\vec{z}^{(k)}(t)$. The rest is exactly the same - including how the gradients are updated, i.e., $\nabla_{\vec{s}}L = (\nabla_{\vec{w}}L \odot Q) \odot \mathbf{1}_{\{0 < \vec{p} < 1\}}$.

2 THEORY

In this section we provide a thorough theoretical analysis of the capabilities of our models, using probabilistic methods and tools from convex random geometry. First, we argue that it is possible to recover Kaiming-He initialisation [9], making the parametrisation of this model comparable to that of arbitrary architectures from a functional perspective. Secondly, we explore the effect of the degree and size parameters $d, n \in \mathbb{N}$. Increasing d provides performance benefits, at the cost of a less sparse matrix. Section 2.1 is dedicated to explaining the performance benefits of d .

LEMMA 2.1. *Let the nonzero entries of the influence matrix Q be distributed as:*

$$q_{i,j} \sim \mathcal{N}\left(0, \frac{6}{dn_i}\right).$$

Let $p_j \sim s\text{-dist}[0, 1]$, $j = 1, \dots, n$, be independent and identically distributed (i.i.d.), where $s\text{-dist}[0, 1]$ is a symmetric distribution with support in $[0, 1]$. Define the vector $\vec{w} = Q\vec{p}$, where each component w_i is given by: $w_i = \sum_{j=1}^n p_j q_{i,j}$. Then, for sufficiently large d , the distribution of w_i converges in distribution to:

$$w_i \xrightarrow{\mathcal{D}} \mathcal{N}\left(0, \mathbb{E}[p_j^2] \frac{6}{n_i}\right),$$

which simplifies to Kaiming-He normal initialization with variance $\sigma^2 = \frac{2}{n_i}$ (where n_i is appropriately chosen for each i) in the case where $p_j \sim U[0, 1]$. In particular, the variance of a neuron with fan-in n_ℓ is then $\text{Var}\left(\text{ReLU}\left(\sum_i^{n_\ell} w_i\right)\right) = 1$.

The proof can be found in the appendix.

2.1 Why large d helps

In practice, Q can be very large and difficult to store in the computer's memory. d controls the sparsity of the matrix; picking a small d maximises the advantages of sparse matrix computation, both in storage and inference. However, a very small d can negatively impact the performance of training. In this section we give a few reasons why larger values of d help. In summary:

- (1) Recall that \mathcal{I}_i the set of non-zero entries in row i of Q with $|\mathcal{I}_i| = d$. The probability that a weight $w_i = Q_i\vec{p}$ is zero is $\prod_{j \in \mathcal{I}_i} (1 - p_j)$, which generally speaking, decreases with d .
- (2) For small values of d , a large proportion of columns (e^{-d}) are entirely zeros. This affects the rank of Q and implies that some entries of \vec{p} become ineffective during training, harming the expressivity of the model.
- (3) Given a matrix Q for any row i ,

$$\max_{\vec{p} \in [0,1]^n} \mathbb{E}\left[|Q_i\vec{p}|\right] = \Theta\left(\sqrt{\frac{d}{n_\ell}}\right),$$

where n_ℓ is the corresponding fan-in value. We prove this in Proposition 2.4. The possibility of large values for \vec{w} leads to increased flexibility in the model, even at the cost of reducing the magnitude of other parameters.

2.1.1 Increasing d decreases the sparsity of \vec{w} .

LEMMA 2.2. *Let $\vec{z} \in \mathbb{R}^n$ be a random vector with $z_j \sim \text{Bern}(U(0, 1))$, and $Q \in \mathbb{R}^{m \times n}$ be the influence matrix. Then the expected number of nonzero entries of $\vec{w} = Q\vec{z}$ is:*

$$\mathbb{E}(\#\text{nonzero entries of } \vec{w}) = m \left(1 - \frac{1}{2^d}\right).$$

PROOF. The j -th element of \vec{w} is given by $w_j = \sum_{k \in S_j} z_k$, where S_j is the set of indices corresponding to the entries of j -th row of Q , with $|S_j| = d$. Let $p_k^* \sim U(0, 1)$; then, the expected value of $P(z_k = 1) = p_k$. Moreover, $\mathbb{E}(p_k) = \frac{1}{2}$. This entails that the probability that all z_k s in S_j are zero is $\frac{1}{2^d}$. Clearly, $P(w_j \neq 0) = 1 - \frac{1}{2^d}$. Summing across the m rows returns the desired result. \square

2.1.2 Small d s lead to inexpressive \vec{p} .

LEMMA 2.3. *The probability that exactly $k \geq 1$ columns of Q are only zeros is given by:*

$$P(k \text{ columns of } Q \text{ are empty}) = \frac{\binom{n}{k} \left(\frac{n-k}{d}\right)^m}{\binom{n}{d}^m}.$$

Moreover, the proportion of empty columns for large $m = n$ is $\approx e^{-d}$.

The proof is in Appendix C. From this probability density function we already see that an increasing d decreases the $\left(\frac{n-k}{d}\right) / \binom{n}{d}^m$ constant. Moreover, in Appendix C, we also show that the expected proportion of empty columns is approximately e^{-d} . For $d = 1$, approximately 36% of columns are empty, meaning that there are only $0.64n$ effective parameters. However, with $d = 10$, the proportion of empty columns is ≈ 0.000045 . Picking a d that is not small significantly increases the expressivity of the model.

2.1.3 Increasing d increases maximum magnitude of w_i .

PROPOSITION 2.4. *For any Q drawn as described in Section 1.3, for any $i \in [m]$, we can find a vector \vec{p} (that depends on Q), such that*

$$\max_{\vec{p} \in [0,1]^n} \mathbb{E}\left[|Q_i\vec{p}|\right] = \Theta\left(\sqrt{\frac{d}{n_\ell}}\right),$$

where n_ℓ is the corresponding fan-in value.

PROOF. Fix an arbitrary row i . Note that $\mathbb{E}\left[q_{i,j} | q_{i,j} > 0\right] = \sigma\sqrt{\frac{2}{\pi}}$ since this is equivalent to the expected value of the half-normal distribution. By symmetry, $\mathbb{E}\left[q_{i,j} | q_{i,j} > 0\right] \leq -\sigma\sqrt{\frac{2}{\pi}}$. Consider Q_i . Assume w.l.o.g there are more positive than negative entries $q_{i,j}$, $j \in [n]$ (otherwise, an analogous argument can be made). For every value $q_{i,j}$ in Q_i that is positive, choose $p_j = 1$ and choose $p_j = 0$ otherwise. Now for the upper bound note that there are at most d positive values and hence $\max_{\vec{p} \in [0,1]^n} \mathbb{E}\left[|Q_i\vec{p}|\right] \leq d\sigma\sqrt{\frac{2}{\pi}}$. Thus, $\max_{\vec{p} \in [0,1]^n} \mathbb{E}\left[|Q_i\vec{p}|\right] \geq \frac{d}{2}\sigma\sqrt{\frac{2}{\pi}}$. Plugging in the value of $\sigma = \sqrt{\frac{6}{dn_\ell}}$ yields the claim. \square

2.2 Compressing by decreasing n

While our approach reduces the communication complexity dramatically, it comes with other tradeoffs in computational costs. There are two reasons that we incur a cost to accuracy.

Firstly, decreasing n leads to fewer effective parameters in the network. This means that weights in \vec{w} propagate their gradients back to fewer \vec{p} , that have to aggregate across gradients of several weights. In particular, a simple calculation shows that: $\mathbb{E}(\text{expected nonzero entries of column } j \text{ in } Q) = \frac{md}{n}$. These can be interpreted as the numbers of parameters that are shared. We see that increasing d and decreasing n both lead to an increase in the expected number of weights affected by one entry of \vec{p} .

Secondly, decreasing n also affects the expressivity of the parameter space. When $n = m$, Q is full rank (provided d is sufficiently large) and the relationship between the weights can be represented by a random linear system $Q\vec{p} = \vec{w}$. However, whenever $n < m$, \vec{p} is projected in a subspace with dimension at most $\dim(Q\vec{p}) = n$.

While increasing the d recovers some of the accuracy, as per Section 2.1, it comes with increased computational costs. Normally, a forward pass takes $\Theta(m)$ operations, one per parameter. Crucially, we work with sparse data structures. In our case, we need to do d multiplications per parameter to calculate the weight vector \vec{w} . Thus, the complexity becomes $\Theta(dm)$. The extra computational costs come from:

- Initialisation: generation of sparse matrix. Algorithm creates d entries per m rows, $O(md)$.
- Forward pass: a sparse CSI vector-matrix multiplication step in each epoch $O(\text{nnz}(n)d) = O(nd)$
- Backpropagation: an extra step in $O(nd)$.

In Section 3.1 we provide evidence of the tradeoff, whereas in Section 3.2 we show that in the federated learning setting the performance costs of n are mitigated. Overall, these costs are offset by the ability to compress the model, which can be very valuable in federated and mobile applications, and the generalisation benefits provided by the framework, which we discuss in the following section.

2.3 Sampling Parameters on Convex Shapes

It is well known that sampling acts as a regularizer and improves the generalisation capabilities of model [25]; in this section we provide a novel theoretical bridge that aims to explain this phenomenon granularly. Indeed, we provide a characterisation of the generalisation capabilities of model through two measures of the probability distribution the model has converged to: the dimension and the volume of the space we explore via sampling.

Specially, we argue two claims. Firstly, that sampling by training improves generalisation, providing a novel link with random convex geometry. To do this we show that the training algorithm is sampling vertices of a geometric shape called a zonotope. We compute the volume of the zonotope explicitly, as an indicator of the volume of the explored space. Secondly, we show that federated learning further improves generalisation by increasing the dimensionality of the space of exploration over which we sample.

Zonotopes are well-studied mathematical objects in convex geometry. Their relevance is already known in deep learning, for instance in the context of describing the expressive power of ReLU

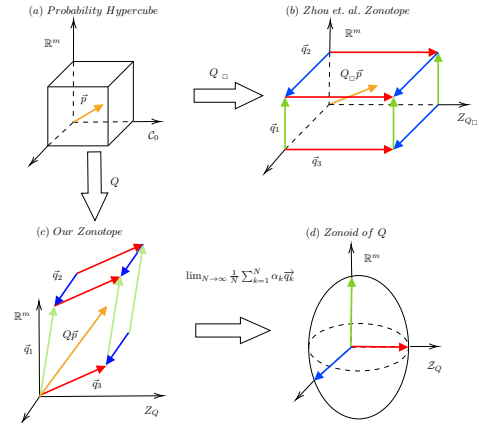


Figure 2: We assume $\mathbb{R}^n = \mathbb{R}^m$ (a) hypercube realised by the possible values of vector \vec{p} , (b) hyperrectangular zonotope generated by the choice of diagonal influence matrix, as in [31], (c) polytopal zonotope generated by our choice of influence matrix, (d) zonoid of the zonotope generated from matrix Q , which yields an ellipsoid.

networks [30]. In this section, we formalise sampling by training through the formalism of subset search on random zonotopes. Specifically, we notice that the influence matrix Q induces a convex shape and characterise training-by-sampling as an exploration of the subset of vertices of the convex shape of interest. Through this intuition, we provide novel insight on the generalisation capabilities of these training methods. This may be the mechanics underpinning the success of approaches stemming from the Lottery Ticket Hypothesis [6], and sampling techniques such as commonly used dropout [25].

Importantly, we show in Section 2.3.2 that there are unique benefits to reap by sampled training in a federated learning setting. Averaging across \vec{p} s of all clients ensures that the dimension of the zonotope that is being explored remains large, even across runs.

2.3.1 Volume: Sampling on Random Zonotopes. The choice of influence matrix Q induces a random convex shape called a *zonotope*. Sampling $Q\vec{z}$ is equivalent to exploring the vertices of this shape. In what follows, we make these statements precise and provide an intuition on how the different choices of parameters (the degree d and size n of the matrix) affect the search space. We refer the interested reader on the calculus of zonoids and their relation to zonotopes to [19].

Definition 2.1 (Random Zonotope). Let $Q = \{\vec{q}_1, \vec{q}_2, \dots, \vec{q}_n\}$, $q_j \sim N(0, \sigma^2)$, $j = 1, \dots, n$ be a collection of random vectors. The random zonotope of Q , Z_Q is the random convex polytope defined by:

$$Z_Q = \left\{ \sum_{j=1}^n \alpha_j \vec{q}_j, \quad \alpha_j \in [0, 1], j = 1, \dots, n \right\}.$$

A zonotope is a specific type of polytope with symmetries in its two dimensional faces [19]. A zonoid is a convex shape, that is not necessary polytopal, that is linked to the expected realisation of a

zonotope. In our case, the zonoid of Q is given by:

$$\mathcal{Z}_Q = \lim_{N \rightarrow \infty} \left\{ \frac{1}{N} \sum_{k=1}^N \alpha_k \vec{q}_k, \alpha_k \in [0, 1], k = 1, \dots, N \right\}. \quad (2)$$

For example, when \vec{q}_j s are standard normal, we have that the zonoid is $\frac{1}{\sqrt{2\pi}} B_n$, where B_n is the unit ball in \mathbb{R}^n . In Figure 2, we provide a visual intuition of the referenced convex shapes and their relationships. This connection to zonoids allows us to compute explicitly the expected volume of a zonotope, which represents the size of region that we sample from in the network's parameter space.

PROPOSITION 2.5. *Let Q be the $n \times n$ influence matrix where each entry $q_{i,j} \sim N(0, 6/dn_i)$. The volume of the zonotope (as in definition 2.1)*

$$\mathbb{E}(\text{vol}_n(\mathcal{Z}_Q)) = \frac{n! (3/d)^{n/2}}{\Gamma(1+n/2)} \prod_{i=1}^n \sqrt{\frac{1}{n_i}}.$$

PROOF. By Vitale's formula [28], we have that:

$$\mathbb{E}(\text{vol}(\mathcal{Z}_Q)) = \mathbb{E} \left(\text{vol}_n \left(\sum_{j=1}^n \vec{q}_j \right) \right) = n! \text{vol}_n(\mathcal{Z}_Q).$$

Using Proposition 5 [18], the zonoid (see Equation (2)) for the matrix ε with i.d.d. columns $\varepsilon_j \sim N(0, 1)$ is: $Z_\varepsilon = \frac{1}{\sqrt{2\pi}} B_n$, where B_n is the n -dimensional ball in \mathbb{R}^n . From Lemma 2 (and as the author also states at the beginning of proof of Theorem 8) [18], it follows that, the zonoid \mathcal{Z}_Q is a linear transformation of the Gaussian ball in \mathbb{R}^n , $Z_Q = B_n \Sigma / \sqrt{2\pi} = B_n \Sigma'$, where $\Sigma^2 = \text{diag}((0, 6/dn_i)_{i=1, \dots, n})$. This is a dispersion ellipsoid; the volume of this object is well known to be:

$$\text{vol}(\mathcal{E}) = \text{vol}(B_n) \det(\Sigma') = \frac{\pi^{n/2}}{\Gamma(1+n/2)} |\det(\Sigma')|,$$

where B_n is the unit ball in \mathbb{R}^n and Γ is the gamma function. The determinant of a square diagonal matrix is given by

$$\det(\Sigma') = \prod_{i=1}^n \sqrt{\frac{6}{2dn_i\pi}} = \left(\frac{3}{d\pi} \right)^{n/2} \prod_{i=1}^n \sqrt{\frac{1}{n_i}},$$

returning the desired output. \square

This applies directly when $d = m = n$ in the influence matrix Q . Increasing the sparsity introduces correlation between the columns of Q , due to how the d non zero elements are selected, while also introducing zeros in the matrix. Therefore we expect the volume to vary in practice; however, we take the theorem to be an indicative value of the size of the ellipsoid in which we sample during training for $d < n$.

2.3.2 Dimension: The Benefits of Federated Learning. Training-by-sampling in [31] is equivalent to exploring the vertices of a rectangular zonotope, which is a hyperrectangle. The distribution on the vertices is updated until one finds an subset of the hyperrectangle where good performance is achieved. In [31], the influence matrix is $Q_\square = \text{diag}(\vec{q})$, $\vec{q} \sim N(0, \Sigma)$, where $\Sigma_{i,i} = \sigma_i^2$, $\Sigma_{i,j} = 0$, $j \neq i$. The supermasks are parametrised by vectors \vec{p} , $p_j \in [0, 1]$, from which we sample: $z_j \sim \text{Bern}(p_j)$, so that $\mathbb{E}[w_\square] = Q_\square \vec{p}$. In otherwords, \vec{z} are

sampled vertices of a hypercube, which are rescaled by randomly initialised weights Q_\square , kept constant in training.

The probability distribution on the vertices of the unit hypercube is given by: $P(\vec{z} = \vec{z}') = \prod_{j=1}^m z'_j p_j + (1 - z'_j)(1 - p_j)$. This leads to: $P(\vec{w} = \vec{w}' | Q_\square = Q'_\square) = \prod_{j=1}^m q'_{j,j} (z'_j p_j + (1 - z'_j)(1 - p_j))$.

Definition 2.2 (τ -Hypercube). Let $C_\tau \subset \mathbb{R}^n$ be a lower dimensional hypercube, given by:

$$C_\tau = \left\{ \vec{\alpha} \odot \vec{\mathbb{I}}(\vec{p}), \sum_{j=1}^n \alpha_j \mathbb{I}_{\{\tau \leq p_j \leq 1-\tau\}}, \tau \in [0, 0.5], \alpha_j \in [0, 1] \right\},$$

where $\vec{\mathbb{I}}(\vec{p}_j) = \mathbb{I}_{\{\tau \leq p_j \leq 1-\tau\}}$, a vector with indicator variables which are 1 if $p_j \in [\tau, 1 - \tau]$ and 0 otherwise.

Note that the expected dimension of this hypercube is at initialisation is:

$$\mathbb{E}(\dim(C_\tau)) = \mathbb{E} \left(\sum_{j=1}^n \mathbb{I}_{\{\tau \leq p_j \leq 1-\tau\}} \right) = n(1 - 2\tau).$$

PROPOSITION 2.6 (BENEFITS OF FEDERATED LEARNING). *Let $\vec{p}_1, \vec{p}_2, \dots, \vec{p}_C$ for a number of clients $C \in \mathbb{N}$, be a collection of vectors, with τ hypercubes given by $C_\tau^{\vec{p}_1}, \dots, C_\tau^{\vec{p}_C}$. Then the hypercube of the average \vec{p} has dimension:*

$$\dim(C_\tau^{\vec{p}}) \geq \frac{1}{C} \sum_{c=1}^C \dim(C_\tau^{\vec{p}_c})$$

PROOF. Let $\#_\tau : \mathbb{R}^n \rightarrow \mathbb{N}$ be the function that counts the number of non-trivial p_i in \vec{p} . This is a convex function; therefore, by Jensen's inequality: $\frac{1}{C} \sum_{c=1}^C \#_\tau(p_{i,c}) \geq \#_\tau \left(\frac{1}{C} \sum_{c=1}^C p_{i,c} \right)$. In other words, the number of non-trivial p_i is larger for averaged p_i s. This directly entails the inequality since $\#_\tau = n - \dim(C_\tau)$. \square

The random zonotope of Q can be expressed as a vector product of sets: $Z_Q = Q C_0 = \{Q\alpha, \alpha \in C_0\}$. Together, Proposition 2.5 and Proposition 2.6 provide insight on what happens during training-by-sampling. At initialisation, we generate an area of exploration via the zonotope of Q , Z_Q . Here, we sample the vertices of Z_Q , with probabilities determined by \vec{p} and compute the loss and gradients with our optimisers. Then, during training, the entries of \vec{p} become extreme: closer to 0 or 1. In turn, this decreases the dimension set of the that we are likely to sample in, which becomes a set of dimension $\dim(C_\tau)$. Our algorithm ensures that we find a set of solutions $S = Q C_\tau$ where there is overall good performance. We show experimentally in Section 3.3 that this leads to drastically improved generalisation compared to training without sampling.

3 EXPERIMENTS

Our experiments complement the theoretical exposition in Section 2, confirming the mathematical claims and showcasing the models' capabilities in the federated setting. The goal of these experiments is to evaluate the performance of LOCAL ZAMPLING and FEDERATED ZAMPLING, as we compress the number of parameters, forcing the weight sharing scheme defined by the matrix Q . The experiments Section 3.1 Section 3.2 provide evidence that the tradeoff between compression and accuracy brought by a choice of small

n can be minimised by using sufficiently large d and deploying the FEDERATED ZAMPLING in the federated setting; Section 3.3 and Appendix B.1 support the claim that LOCAL ZAMPLING alone can provide benefits in generalisation and performance, even compared to [31].

Experiment Summary. We run four experimental evaluations. First we show the tradeoff between compression factor and performance across different d s in Section 3.1. As predicted from the theory, increasing d s marginally above 1 increases the accuracy. In this experiment we explore the effect of compression.

Second, we test our framework in the federated learning setting applying compression. We run three simulations showing that a factor 32x compression on architecture size (and 1024x compression against the standard case). This provides evidence of the benefits of sampling in presented in Section 2.3.

Third, we run our experiments to showcase the generalisation properties of our approach. We do this by perturbing \vec{p} across the dimensions where $\tau < p_j < 1 - \tau$ by a Gaussian impulse. We provide evidence of robustness of the LOCAL ZAMPLING’s accuracy to strong perturbations \vec{p} when compared to training the expected network (i.e. training without sampling). As predicted in Section 2.3, perturbing the non-trivial entries of \vec{p} of the model leads to minimal effect on the network performance, supporting the view that our framework finds regions of strong generalisation.

Finally, we show evidence that our model is superior to Zhou et. al. [31]. Over very few runs, we show clear advantages in using LOCAL ZAMPLING across all choices of d . We believe this is due to the benefits induced by a larger d Section 2.1 and the generalisation benefits described in Section 2.3.

Experimental Constant. We report the experimental choices that were present in all experiments to avoid repetition. More detail for each experiments is reported in each section. The evaluation of basic method was run on a machine with GPU RTX3080 with 12GBs of VRAM, with AMD Ryzen Threadripper 3960X 24-Core CPU and RAM 256GBs. In all our experiments we use the MNIST dataset and use the framework described in Section 1.3. We run each training round for 100 epochs with early stopping, using 10 epochs of patience and a delta of 10^{-4} . All our training is run using Adam optimizer, with momentum 0.9 and varying learning rate. Everywhere, we use the standard MNIST data splits with batches of size 128. The model’s parameter initialization followed a uniform distribution on \vec{p} and we choose $q_{i,j}$ to be distributed as in Lemma 2.1, to recover Kaiming-He initialisation. The code is reproducible and shared at [github.anon.com](https://github.com/anon.com), using PyTorch.

We use one of two architectures in each of our experiments: SMALL ARCHITECTURE or MNISTFC. Our compression experiments Section 3.1 and sensitivity Section 3.3 experiments we use SMALL ARCHITECTURE, which is a feedforward neural networks with two hidden layers and twenty neurons per layer. The MNISTFC is exactly as the one in Zhou, two hidden layers with three hundred and one hundred neurons respectively. This architecture is used both in the federated setting Section 3.2 and in comparison with [31], in Appendix B.1.

3.1 Varying the Compression Factor m/n

Setup. In this experiment we vary the compression factor in the LOCAL ZAMPLING.⁷ The goal of this experiment is to see the impact n plays on the accuracy. We train architectures with for 5 levels of $d = 1, 5, 10, 50, 100$ and with compression factor 11 levels of $m/n = 2^i, i = 0, \dots, 10$ reported in Figure 3. For each architecture, we run 5 random seeds (seed = 0,...,4) with learning rate 0.001. After a training round, we sample 100 networks and compute mean sampled accuracy. We report the average of the sampled accuracy and the standard deviation in the Figure 3.

Analysis. We see in Figure 3 the trade-off between the compression factor and the accuracy. It appears that increasing d beyond 5 makes little difference, which tracks with the mathematical of impact we discuss in Section 2.1. For $d = 1$ the results are consistently worse. The expected accuracy ($\vec{w}^* = Q\vec{p}^*$, where \vec{p}^* is the final probability vector) overall is almost the same as the sampled accuracy ($\vec{w}^* = Q\vec{z}^*$, with $\vec{z}^* \sim \vec{p}^*$). The accuracy seems to follow roughly inverted logarithmic trend, i.e., doubling the compression factor leads to a constant drop. In particular, for $d = 5$ we see that a $m/n = 4$ results in a drop of about on average 5 with the standard deviation being of about the same order of magnitude. The values of the experiment can be found in Appendix B.

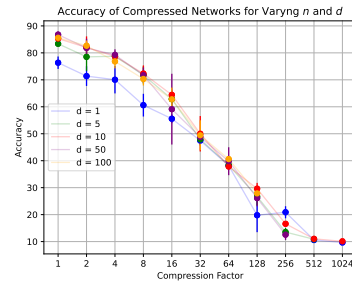


Figure 3: Trade-off between compression and accuracy SMALL ARCHITECTURE in LOCAL ZAMPLING for varying levels of d .

3.2 Federated Learning Experiments

Setup. In the federated learning setup, we ran three simulations with 10 clients and one server. Each client was trained over a total of 100 rounds. The data was partitioned with a random split. In this experiment, we tested the MNISTFC model with training-by-sampling, measuring the accuracy on the expected network. The model was initialized with $n = m/i, i = 1, 8, 32$, where $m = 266610$ and a $d = 10$, with \vec{p} initialized uniformly and learning rate is 0.1, random seed is 1. We compute the mean sampled accuracy at each round, together with the standard deviation out of 100 sampled networks.

Analysis. Results are displayed in Section 3.2. Bench-marking against $m/n = 1$, we see that our performance gets virtually no loss in performance (.22%) for a 8 fold reduction in parameters in

⁷Running the experiment in the LOCAL ZAMPLING allows us to isolate that impact of the compression rate, with no impact coming from the averaging binary numbers (recall that in FEDERATED ZAMPLING the clients sends binary numbers).

the $m/n = 8$ experiment. Moreover, in the $m/n = 32$ compression experiment, we recover (2.55%). The metrics are summarised in Section 3.2 and compared to [13].

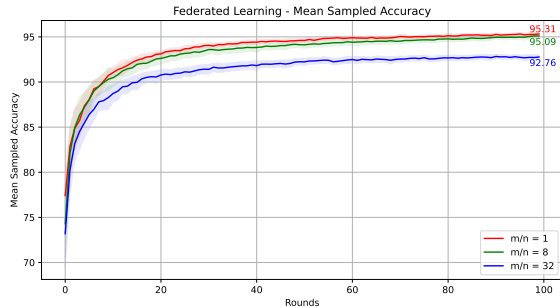


Figure 4: Results of training FEDERATED ZAMPLING in the federated learning framework with varying levels of d .

Comparing the 1,933,258 parameter ConvNet architecture in Isik et. al. [13], we use a 266,610 parameter feedforward (about 7 times smaller) architecture. The clusters we have access to were unable to run their architecture, which is why we only have a test accuracy of 0.95 (instead of their 0.99) even without compression. We believe that our results on their architecture would result in even higher accuracies and with higher compression factors due to their model being much more over-parameterised.

3.3 Generalisation Properties via Parameter Sensitivity

Setup. This experiments aims to verify the claims in Section 2.3 pertaining to the generalisation capabilities. We claimed that the network finds a convex subspace of \mathbb{R}^m where there is good performance. To validate our claims, we train LOCAL ZAMPLING under two regimes: either via sampling or via Adam on $\vec{w} = Q\vec{p}^*$. For each we compute performance by perturbing the final learned vector \vec{p} by an ϵ_τ , where $\epsilon_{\tau,i} \sim N(0, 1)$ whenever $\tau \leq p_j \leq 1 - \tau$ and is 0 otherwise. Performance is computed across 10 perturbations and averaged. We compute mean sampled accuracy (across 10 sampled networks) and accuracy for the respective methods. We then compute the average sensitivity (change in performance divided by initial performance) and average deviation (change in performance divided by the

	client savings	server savings	test accuracy
[13]	33.69 (*)	1.05 (*)	0.99
[us] $m/n = 8$	256	8	0.95
[us] $m/n = 32$	1024	32	0.93

Table 1: All savings are measure by what factor the communication cost decreases per round in comparison to the naive protocol that sends all m parameters as floats. For example, just sends a bit rather than a float results in 32. (*) The bit-rate they achieved was about 0.95 due to arithmetic compression. Note that they use a larger architecture (about 7 times larger).

L2 norm of ϵ_τ). We report the standard deviation across the 10 measurements.

Analysis. We display the results in Table 4. Overall, the clear trend is that the sampled network both performs better and witnesses average sensitivity and deviation smaller by two orders of magnitude, signalling the generalisation benefits of training-by-sampling. Moreover, even when $\tau = 0.5$ (and therefore all values p_j are perturbed), we see a gap in robustness between training-by-sampling and traditional training of the expected network: an 11% drop versus a 62% drop in performance.

4 CONCLUSIONS

We introduced a new framework capable of learning on a compressed parameter space while maintaining remarkable accuracy in the federated learning setting. Importantly, we introduced a novel link between random convex geometry and training-by-sampling, which we expect will lead to new insight into probabilistic training of networks. Using zonotope calculus, we characterize the sample space of our compressed network and we establish properties regarding the volume and dimensions of the sample space. We hope this new perspective on generalisation and the *density of good solutions* in the parameter space.

While this work focuses mostly on the *silos* federated learning setting (where one central server receives and spreads messages from clients), we envision future work to focus on a distributed setting, without a central server, testing the performance of FEDERATED ZAMPLING where the communication between clients follows arbitrary graph patterns. On the other hand, further theoretical analysis might give insights into the relationship between the weight sharing literature, for instance, a direct comparison with works such as [5].

Finally, in Section 3.3 we have shown that some entries of \vec{p} are not influential in the forward pass of the model. This suggests that further compression of (Q, \vec{p}) can be achieved, without loss of accuracy. Specifically, we can remove the columns of Q related to trivial \vec{p} s, and reduce the rows of Q when weights are summed to 0. We conjecture this will decrease further the communication cost in the federated learning setting.

REFERENCES

- [1] Alham Fikri Aji and Kenneth Heafield. 2017. Sparse communication for distributed gradient descent. *arXiv preprint arXiv:1704.05021* (2017).
- [2] Leighton Pate Barnes, Huseyin A Inan, Berivan Isik, and Ayfer Özgür. 2020. rTop-k: A statistical estimation approach to distributed SGD. *IEEE Journal on Selected Areas in Information Theory* 1, 3 (2020), 897–907.
- [3] Ran Ben Basat, Shay Vargaftik, Amit Portnoy, Gil Einziger, Yaniv Ben-Itzhak, and Michael Mitzenmacher. 2022. QUIC-FL: Quick Unbiased Compression for Federated Learning. *arXiv preprint arXiv:2205.13341* (2022).
- [4] Clément Louis Canonne, Venkatesan Guruswami, Raghu Meka, and Madhu Sudan. 2015. Communication with imperfectly shared randomness. In *Proceedings of the 2015 Conference on Innovations in Theoretical Computer Science*. 257–262.
- [5] Wenlin Chen, James Wilson, Stephen Tyre, Kilian Weinberger, and Yixin Chen. 2015. Compressing neural networks with the hashing trick. In *International conference on machine learning*. PMLR, 2285–2294.
- [6] Jonathan Frankle and Michael Carbin. 2018. The Lottery Ticket Hypothesis: Finding Sparse, Trainable Neural Networks. In *International Conference on Learning Representations*.
- [7] Advait Harshal Gadghikar, Sohom Mukherjee, and Rebekka Burkholz. 2023. Why Random Pruning Is All We Need to Start Sparse. (June 2023).
- [8] Andrew Hard, Kanishka Rao, Rajiv Mathews, Swaroop Ramaswamy, Françoise Beaufays, Sean Augenstein, Hubert Eichner, Chloé Kiddon, and Daniel Ramage. 2018. Federated learning for mobile keyboard prediction. *arXiv preprint arXiv:1811.03604* (2018).
- [9] Kaiming He, Xiangyu Zhang, Shaoqing Ren, and Jian Sun. 2015. Delving deep into rectifiers: Surpassing human-level performance on imagenet classification. In *Proceedings of the IEEE international conference on computer vision*. 1026–1034.
- [10] Liam Hebert, Lukasz Golab, Pascal Poupart, and Robin Cohen. 2023. FedFormer: Contextual Federation with Attention in Reinforcement Learning. In *Proceedings of the 22nd International Conference on Autonomous Agents and Multiagent Systems (AAMAS)*.
- [11] Berivan Isik, Wei-Ning Chen, Ayfer Ozgur, Tsachy Weissman, and Albert No. 2024. Exact optimality of communication-privacy-utility tradeoffs in distributed mean estimation. *Advances in Neural Information Processing Systems* 36 (2024).
- [12] Berivan Isik, Francesco Pase, Deniz Gunduz, Sanmi Koyejo, Tsachy Weissman, and Michele Zorzi. 2024. Adaptive Compression in Federated Learning via Side Information. In *Proceedings of The 27th International Conference on Artificial Intelligence and Statistics*. PMLR, 487–495.
- [13] Berivan Isik, Francesco Pase, Deniz Gunduz, Tsachy Weissman, and Zorzi Michele. 2023. Sparse Random Networks for Communication-Efficient Federated Learning. In *The Eleventh International Conference on Learning Representations*.
- [14] Berivan Isik, Tsachy Weissman, and Albert No. 2022. An information-theoretic justification for model pruning. In *International Conference on Artificial Intelligence and Statistics*. PMLR, 3821–3846.
- [15] Jakub Konečný, Brendan McMahan, and Daniel Ramage. 2015. Federated optimization: Distributed optimization beyond the datacenter. In *8th NIPS Workshop on Optimization for Machine Learning*. <https://opt-ml.org/oldopt/opt15/papers.html>
- [16] Gowtham R Kurri, Vinod M Prabhakaran, and Anand D Sarwate. 2021. Coordination through shared randomness. *IEEE Transactions on Information Theory* 67, 8 (2021), 4948–4974.
- [17] Yujun Lin, Song Han, Huizi Mao, Yu Wang, and William J Dally. 2018. Deep Gradient Compression: Reducing the Communication Bandwidth for Distributed Training. In *International Conference on Learning Representations (ICLR)*.
- [18] Leo Mathis. 2022. Gaussian Zonoids, Gaussian determinants and Gaussian random fields. *arXiv preprint arXiv:2203.00651* (2022).
- [19] Leo Mathis. 2022. The handbook of zonoid calculus. (2022).
- [20] Brendan McMahan, Eider Moore, Daniel Ramage, Seth Hampson, and Blaise Aguerre y Arcas. 2017. Communication-efficient learning of deep networks from decentralized data. In *Artificial intelligence and statistics*. PMLR, 1273–1282.
- [21] Hikari Otsuka, Daiki Chijiwa, Ángel López García-Arias, Yasuyuki Okoshi, Kazushi Kawamura, Thiem Van Chu, Daichi Fujiki, Susumu Takeuchi, and Masato Motomura. 2024. Partial Search in a Frozen Network Is Enough to Find a Strong Lottery Ticket. <https://doi.org/10.48550/arXiv.2402.14029> arXiv:2402.14029 [cs, stat]
- [22] Ankit Pensia, Shashank Rajput, Alliot Nagle, Harit Vishwakarma, and Dimitris Papailiopoulos. 2020. Optimal Lottery Tickets via SUBSETSUM: Logarithmic over-Parameterization Is Sufficient. In *Proceedings of the 34th International Conference on Neural Information Processing Systems (NIPS’20)*. Curran Associates Inc., Red Hook, NY, USA, 2599–2610.
- [23] Vivek Ramanujan, Mitchell Wortsman, Aniruddha Kembhavi, Ali Farhadi, and Mohammad Rastegari. 2020. What’s Hidden in a Randomly Weighted Neural Network?. In *2020 IEEE/CVF Conference on Computer Vision and Pattern Recognition (CVPR)*. 11890–11899. <https://doi.org/10.1109/CVPR42600.2020.01191>
- [24] Vivek Ramanujan, Mitchell Wortsman, Aniruddha Kembhavi, Ali Farhadi, and Mohammad Rastegari. 2020. What’s Hidden in a Randomly Weighted Neural Network?. In *2020 IEEE/CVF Conference on Computer Vision and Pattern Recognition (CVPR)*. 11890–11899. <https://doi.org/10.1109/CVPR42600.2020.01191>
- [25] Nitish Srivastava, Geoffrey Hinton, Alex Krizhevsky, Ilya Sutskever, and Ruslan Salakhutdinov. 2014. Dropout: A simple way to prevent neural networks from overfitting. *Journal of machine learning research* 15, 1 (2014), 1929–1958.
- [26] Lucas Theis, Tim Salimans, Matthew D Hoffman, and Fabian Mentzer. 2022. Lossy compression with gaussian diffusion. *arXiv preprint arXiv:2206.08889* (2022).
- [27] Authors Unknown. 2024. Fuzzy Clustered Federated Learning Under Mixed Data Distributions. In *Proceedings of the 23rd International Conference on Autonomous Agents and Multiagent Systems (AAMAS)*.
- [28] Richard A Vitale. 1991. Expected absolute random determinants and zonoids. *The Annals of Applied Probability* 1, 2 (1991), 293–300.
- [29] Hongyi Wang, Scott Sievert, Shengchao Liu, Zachary Charles, Dimitris Papailiopoulos, and Stephen Wright. 2018. Atomo: Communication-efficient learning via atomic sparsification. *Advances in neural information processing systems* 31 (2018).
- [30] Liwen Zhang, Gregory Naitzat, and Lek-Heng Lim. 2018. Tropical geometry of deep neural networks. In *International Conference on Machine Learning*. PMLR, 5824–5832.
- [31] Hattie Zhou, Janice Lan, Rosanne Liu, and Jason Yosinski. 2019. Deconstructing Lottery Tickets: Zeros, Signs, and the Supermask. *NIPS* (2019), 11.

A INITIALISATION

In this section we study the impact of different initialization. Concretely we study how the network performance changes if we train the values \vec{p} directly, without sampling, i.e., we compute the gradient w.r.t. to \vec{p} rather than not \vec{z} . We run this experiment on the MNISTFC, by training the $Q\vec{p}$ traditionally (without sampling). We use a learning rate of 0.01 and change initialisation according to the parameters of a beta distribution. We take the average over 3 random seeds. We display the results in Figure 5.

The blue line at the top represents the test accuracy of the expected network, given by $\vec{w} = Q\vec{p}$ (without sampling). We see that whenever we sample a $\vec{z} \sim \text{Bern}(\vec{p})$, the performance of the network collapses, contrary to what is witness when the neural network is trained via sampling, where the difference between sampled and expected network performance is small. We refer to this difference as the *integrality gap*.

Changing initialisation strongly affects the behaviour of the model. Small beta parameters imply that the distribution of \vec{p} has high density around 0 and 1. This artificially decreases the decreases the integrality gap, making the red and blue performance curves closer to each other. As we increase the beta parameters, the two curves diverge. We conjecture that this is the case because the parameters stay close to their initial distribution when training without sampling: this entails that the difference between \vec{z} and \vec{p} is small at initialisation and remains small throughout training whenever then beta parameters are around 1/10. We also see that for small beta parameters the variance and max-min gap of the performance of sampled networks (from 100 samples) is minimised. Again, this is because the extreme \vec{p} s force the \vec{z} s to specific values (either 0 or 1) with high probability.

We also plot the curve of the discretized network. This is a network with \vec{p}_o , where $p_{o,j} = \text{argmin}_{z=0,1} |p_j - z|$. Interestingly, the performance of the discretized network is enveloped around the curve of the expected and sampled networks for small beta parameters. However, as we increase the distribution’s parameters, we find that the discretised network performs worse than the mean sampled network. This is because the values of \vec{p} are increasingly

distributed around 1/2 and the discretization moves the network far from the learned parameters.

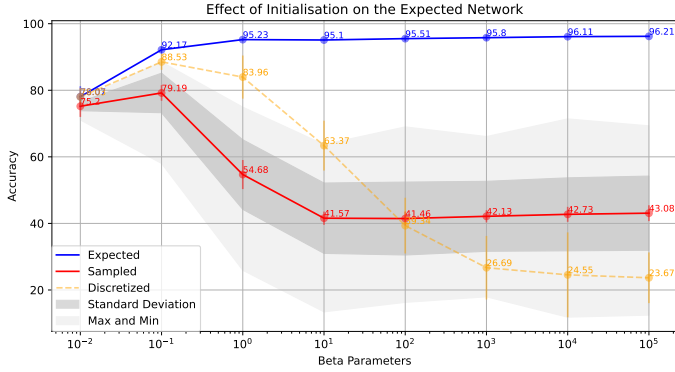


Figure 5: In this figure we study the impact training-by-sampling has. The figures shows that if we only train the \vec{p} directly and then sample a network in the end, it is not robust. However, selecting initialization that have abundant extreme values, decreases the integrality gap.

B EXTENDED RESULTS: SECTION 3.1

When you perturb all values of \vec{p} indiscriminately ($\tau = 0.5$), performance decreases marginally for sampled networks, but collapses for networks trained regularly.

B.1 Comparison with Zhou et. al. [31]

Setup. For our comparison with Zhou et. al [31] we aimed to contrast our performance of LOCAL ZAMPLING against the aforementioned approach by varying the degree of Q in powers of 2 ($d = 2, 4, 16, 256$). We run each experiment on 5 random seeds, training the model with a learning rate of 0.001. We sampled on 100 networks at the end of training and capture the best performance (as in [31], providing the standard deviation across the random seeds).

Analysis. This setup aimed to evaluate the effectiveness of LOCAL ZAMPLING under conditions similar to those used in Zhou’s work, providing a basis for direct comparison. Appendix B.1 provides evidence that our method easily performs better than the supermask approach in [31]. Interestingly, we verify the benefits in increasing to very large values ($d = 256$), beyond avoiding small values of d . We conjecture this is due to the reasons provided in Section 2.1.

C MISSING PROOFS

PROOF OF LEMMA 2.3. (Recall that $k \leq d \leq n$). The number of possible ways to choose $k \geq 1$ columns is $\binom{n}{k}$. Once these have been chosen there are $\binom{n-k}{d}$ ways to fill the row of the column without selecting the k entries that need to empty. This needs to be repeated m time, for each row, so that:

$$\#(\text{Number of acceptable configurations of } Q) = \binom{n}{k} \binom{n-k}{d}^m.$$

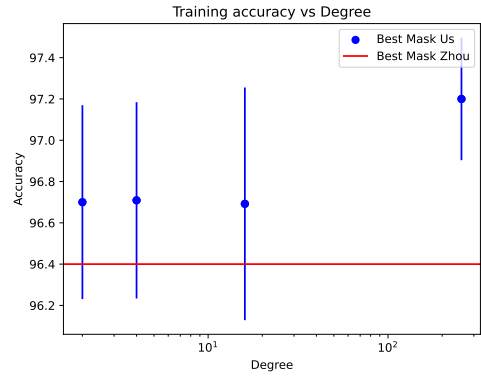


Figure 6: Comparison between our method for different degrees d and Zhou et. al. [31]; best mask refers to the best sampled \vec{z} .

The total number of ways to pick d entries out of m in m rows is:

$$\#(\text{Total configurations of } Q) = \binom{n}{d}^m.$$

This entails that: $P(k \text{ columns of } Q \text{ are empty}) = \frac{\binom{n}{k} \binom{n-k}{d}^m}{\binom{n}{d}^m}$.

We proceed to show that the number of zero columns in $\approx e^{-d}$. By combinatorial argument, for each row, the probability that a specific column is not selected is:

$$P(\text{column } j \text{ not selected in one row}) = \binom{n-1}{d} \binom{n}{d}^{-1}.$$

$$\binom{n-1}{d} \binom{n}{d}^{-1} = \frac{(n-1)!(n-d)!}{n!(n-1-d)!} = \frac{n-d}{n}.$$

Since each row is independent, the probability that the column is empty across all m rows is:

$$P(\text{column } j \text{ is empty}) = \left(\frac{n-d}{n}\right)^m$$

An approximation for the expected number of empty columns (assuming independence of columns) is given by:

$$\mathbb{E}(\#(\text{empty columns})) \approx n \left(1 - \frac{d}{n}\right)^m$$

which, for large $n = m \gg d$ reduces to: $\mathbb{E}(\#(\text{empty columns})) \approx me^{-d}$. \square

We also have that:

$$\begin{aligned} \mathbb{E}(\text{expected nonzero columns of } Q) &= \sum_{k=1}^n k \frac{\binom{n}{k} \binom{n-k}{d}^m}{\binom{n}{d}^m} \\ &= \frac{1}{\binom{n}{d}^m} \sum_{k=1}^d k \binom{n}{k} \binom{n-k}{d}^m. \end{aligned}$$

Whereas, the probability that there are no non-zero columns is:

$$\begin{aligned} P(Q \text{ has no nonzero columns}) &= 1 - \sum_{i=1}^d \frac{\binom{n}{k}}{\binom{n}{d}^m} \binom{n-k}{d}^m \\ &= 1 - \binom{n}{d}^{-m} \sum_{i=1}^d \binom{n}{k} \binom{n-k}{d}^m. \end{aligned}$$

In general, these quantities are really small: most of the genes are effective populated. Moreover, notice that expected number of nonzero elements for a row is:

$\mathbb{E}(\text{expected nonzero entries of column } j \text{ in } Q) = \frac{md}{n}$. This quantity can be interpreted as the expected number of weights influenced by a gene. Smaller n implies a gene has a greater influence on the weights. Larger d also makes all genes affect a larger number of weights.

PROOF OF LEMMA 2.1. Since p_j and $q_{i,j}$: $\mathbb{E}[p_j q_{i,j}] = \mathbb{E}[p_j] \cdot \mathbb{E}[q_{i,j}] = 0$. Thus, the expected value of w_i is:

$$\mathbb{E}[w_i] = \mathbb{E} \left[\sum_{j=1}^n p_j q_{i,j} \right] = \sum_{j=1}^n \mathbb{E}[p_j q_{i,j}] = 0.$$

Next, we calculate the variance of w_i . Since the $q_{i,j}$'s are independent normal random variables, the variance of w_i is the sum of the variances of the individual terms $p_j q_{i,j}$: $\text{Var}(w_i) = \sum_{j=1}^n \text{Var}(p_j q_{i,j})$. Using the fact that p_j and $q_{i,j}$ are independent, we can write: $\text{Var}(p_j q_{i,j}) = \mathbb{E}[p_j^2] \cdot \text{Var}(q_{i,j}) = \mathbb{E}[p_j^2] \cdot \frac{6}{dn_i}$. Thus, the total variance of w_i is: $\text{Var}(w_i) = \sum_{j=1}^n \mathbb{E}[p_j^2] \cdot \frac{6}{dn_i} = d \cdot \mathbb{E}[p_j^2] \cdot \frac{6}{dn_i}$. By the Central Limit Theorem, since w_i is the sum of d independent random variables, and each $p_j q_{i,j}$ has mean 0 and finite variance, for large d , the distribution of w_i converges to a normal distribution:

$$w_i \xrightarrow{\mathcal{D}} \mathcal{N} \left(0, \mathbb{E}[p_j^2] \cdot \frac{6}{n_i} \right).$$

If $p_j \sim U[0, 1]$, then $\mathbb{E}[p_j^2]$ is the second moment of the uniform distribution on $[0, 1]$. The second moment of $U[0, 1]$ is:

$$\mathbb{E}[p_j^2] = \int_0^1 p_j^2 dp_j = \frac{1}{3},$$

which yields Kaiming-He normal distribution. \square

Table 2: Mean Sampled Accuracy for Different d s and Compression Factors m/n .

Weight degree d	Compression Factor					
	1	2	4	8	16	32
100	85.60 ± 2.16	82.63 ± 2.43	76.83 ± 2.93	70.33 ± 2.98	62.78 ± 3.29	49.43 ± 3.32
50	86.77 ± 1.76	81.83 ± 2.30	79.28 ± 2.76	71.75 ± 2.94	59.12 ± 3.71	48.76 ± 3.59
10	85.29 ± 2.20	81.99 ± 2.50	78.70 ± 2.56	72.31 ± 2.90	64.43 ± 2.65	49.99 ± 2.99
5	83.37 ± 2.42	78.52 ± 3.40	78.73 ± 2.81	71.80 ± 3.17	62.85 ± 3.02	47.90 ± 3.33
1	76.35 ± 3.21	71.37 ± 4.25	70.05 ± 3.55	60.60 ± 3.49	55.56 ± 3.54	47.48 ± 3.00

Table 3: This plot shows our accuracy with varying compression rate n/m . A rate of 1 means no compression and a rate of $1/r$ compresses the model by a factor of r .**Table 4: Table presenting random sampling in the C_τ hypercubes for networks trained via sampling versus regular training.**

τ	Average Accuracy		Average Sensitivity		Average Deviation	
	Regular	Sampled	Regular	Sampled	Regular	Sampled
0.01	82.85 ± 2.82	90.29 ± 0.64	0.13 ± 0.03	$(3.52 \pm 1.61) \times 10^{-3}$	0.09 ± 0.02	$(2.50 \pm 1.13) \times 10^{-3}$
0.10	81.43 ± 4.01	89.67 ± 0.90	0.14 ± 0.04	$(3.04 \pm 0.93) \times 10^{-3}$	0.10 ± 0.03	$(2.13 \pm 0.65) \times 10^{-3}$
0.20	82.42 ± 3.77	89.64 ± 1.12	0.13 ± 0.04	$(2.17 \pm 0.92) \times 10^{-3}$	0.10 ± 0.03	$(1.52 \pm 0.63) \times 10^{-3}$
0.50	20.07 ± 0.99	78.80 ± 3.28	0.78 ± 0.01	0.17 ± 0.03	0.55 ± 0.01	0.12 ± 0.02